Diffraction studies of the (222) reflection in Ge and Si: Anharmonicity and the bonding electrons*

J. B. Roberto and B. W. Batterman
Department of Materials Science and Engineering, Cornell University, Ithaca, New York 14850

D. T. Keating
Brookhaven National Laboratory, Upton, New York 11973

(Received 24 October 1973)

We present the results of a combined x-ray and neutron diffraction study of the temperature dependence of the "forbidden" (222) reflection in germanium. Integrated intensities were measured from room temperature to 850°C with x rays and to 904°C with neutrons. In addition, an earlier x-ray study of the silicon (222) reflection has been improved and extended to 800°C and a correction has been made in the corresponding neutron results. The germanium and silicon data are interpreted in terms of anharmonic atomic vibrations and anticentrosymmetric valence-charge distributions. Contrary to our previous reports, the temperature dependence of the scattering from the bonding electrons is found to be similar to that from the core electrons.

I. INTRODUCTION

Silicon and germanium crystallize in the diamond structure, which is characterized by two interpenetrating fcc sublattices displaced by one quarter of the distance along the cube diagonal. Each unit cell contains two atomic positions which can be denoted A and B. Each atom has tetrahedral site symmetry, but the atomic positions at A and B are related by inversion symmetry. As a result, the structure factor for the unit cell $F(222)$ can be written $F(222) = 4(f_A - f_B)$, where f_A and f_B are the Fourier transforms of the distributions of scattering matter at A and B. It is easily seen that identical centrosymmetric atoms placed at A and B positions would yield a vanishing structure factor at the (222) position in diamond cubic crystals.

The distribution of scattering matter in diamond-structured crystals, however, need not be centrosymmetric. In fact, any perturbation of the atoms reflecting their tetrahedral site symmetry will add an anticentrosymmetric component to the distribution of scattering matter, yielding a nonzero $F(222)$. One such perturbation is due to the tetrahedral orientation of the covalent bonds in these crystals, and has long been recognized as the primary contribution to the weak intensity observed with x-rays at the forbidden (222) position in diamond.[1] More recently, it has been suggested that the mean atomic-site potentials also have tetrahedral symmetry,[2] resulting in a weak (222) reflection due to anharmonic atomic motions. The anharmonic effect has been recently detected with neutrons in silicon[3] and germanium.[4]

Neutrons interact primarily with the point nucleus, and hence neutron measurements at the (222) are sensitive essentially to only the anharmonic nuclear vibrations. X-ray measurements, on the other hand, interact with the electronic charge distributions of the atoms, and are thus sensitive to both the covalent bonds and to the anharmonic motions of the core electrons. The anharmonic behavior of the core electrons and the nucleus should be the same, since the atom core and nuclei are expected to vibrate as a whole. As a result, anharmonic effects measured with neutrons can be used to determine the anharmonic contribution in the x-ray data, yielding a determination of the scattering from the bonds themselves. Intuitive arguments suggest that the bonding and anharmonic contributions to the x-ray (222) intensity should be of opposite sign.[3,5] This has been recently confirmed by experiment.[6]

In this paper, we report the results of a combined x-ray and neutron study of the temperature dependence of the (222) reflection in germanium. During the course of the study, several experimental difficulties were encountered which also had a bearing on our earlier silicon results.[3,5] Accordingly, the updated silicon data is also presented here. When discussed along with the new high-temperature silicon x-ray measurements, these updated results lead to revised conclusions concerning the anharmonic and bonding characteristics of silicon. In particular, it is found that the temperature dependence of the valence-charge scattering in both germanium and silicon is similar to that of the core electrons.

II. NEUTRON EXPERIMENT AND RESULTS

The forbidden (222) neutron reflection in germanium was detected and its temperature dependence measured from 23 to 904 °C. The experimental technique generally followed that of Keating *et al.*[3] in their measurement of the silicon (222) and will be discussed in detail only in those areas

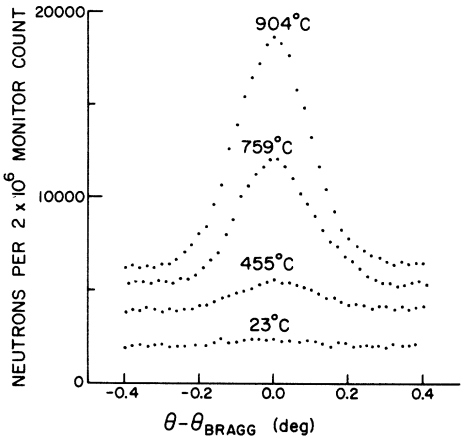

FIG. 1. Characteristic θ scans used to determine the relative neutron Ge(222) integrated intensities from 23 to 904 °C. The increase of the background with absolute temperature is linear, as would be expected from first-order thermal diffuse scattering.

unique to the germanium measurement.

In both germanium and silicon the anharmonic effects are extremely weak. The resulting intensities are very small, and great care must be exercised to exclude contributions at the (222) from multiple-diffraction effects and harmonic-wavelength contaminants in the neutron beam. Extinction effects in the diffraction process are also potentially significant.

The measurements were carried out on large-volume single crystals of germanium at the Brookhaven High Flux Beam Reactor. Relative intensities of the germanium (222) were measured at each temperature using θ scans with 20′ horizontal collimators at the counter to increase the signal-to-noise ratio. These intensities were then normalized to absolute-intensity measurements at the two highest temperatures where increased thermal motion greatly increased the anharmonic effects. This dramatic rise in (222) intensity as temperature is increased is seen in Fig. 1. The primary-beam intensity was directly measured by means of known boron-glass absorbers. This was checked by measuring the (111) integrated intensities of two perfect silicon crystals of different thicknesses and using dynamical theory to compute the incident intensity. All three measurements agreed to 5%.

The possible excitation of multiple Bragg events at the (222) position was carefully avoided by the appropriate choice of wavelength and crystal azimuthal position. The positions of both "Umweganregung" and "Aufhellung" conditions[7] are readily computed using the techniques of Cole *et al.*[8] In our case, a combination of $\lambda = 2.366$ Å and $\phi = 23°$ yielded a region free of simultaneous diffraction effects. In Fig. 2 we plot the loci of possible simultaneous reflections at the germanium (222) along with the approximate extent of our resolution function.

We used a graphite monochromator diffracting from the (002) planes. This provided an intense primary beam (approximately 9.0×10^5 neutron/sec cm^2) but also included substantial contributions from the short-wavelength harmonics $\lambda/2$, $\lambda/3$, etc. The use of 15 cm of tuned pyrolytic graphite filters[9] placed after the monochromator and before the sample was essential in eliminating the possible harmonic contributions. At $\lambda = 2.366$ Å, the filters are extremely efficient in removing these short-wavelength harmonics, particularly the dominant $\lambda/2$ component. With the filters in position, no diffracted beam could be detected at the (111) position for $\lambda/2$, $\lambda/3$, and $\lambda/4$. In addition, the purity of the beam was checked over four orders of magnitude with known boron-glass absorbers which have wavelength-dependent attenuations.

The temperature dependence of the germanium (222) reflection was first measured in symmetric Bragg reflection with a low-dislocation-density germanium crystal. At each temperature, the

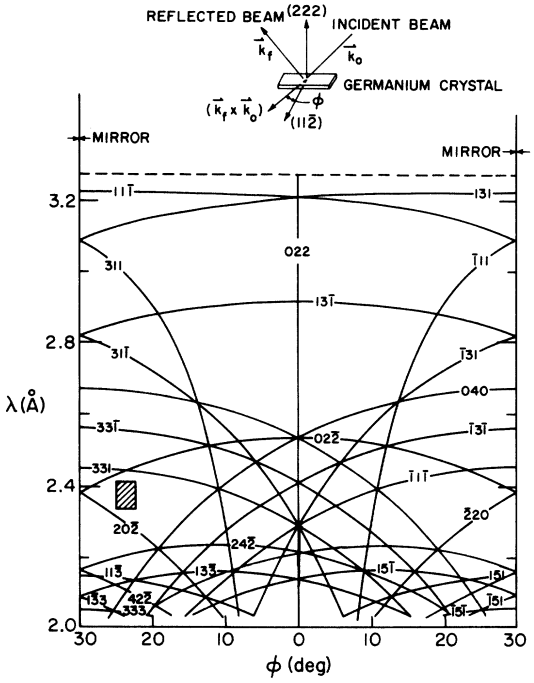

FIG. 2. Azimuthal position of simultaneous diffraction events at the Ge(222) plotted as a function of neutron wavelength. Both "Umweganregung" and "Aufhellung" conditions (odd and even indices, respectively) are indicated. The approximate extent of our resolution function is depicted by the rectangle at $\Phi = 23°$, $\lambda = 2.366$ Å.

θ position of the (222) reflection was carefully determined by removing the filters and locating the $\lambda/2$ peak from the (444) reflection, which occurs at θ (222). The filters were then replaced and the (222) diffracted intensity measured. A 1.50-cm-high-by-0.75-cm-wide slit was placed before the sample in the relative θ-scan measurements. This was the maximum slit size commensurate with the size of the sample, the 20′ in pile horizontal collimation, the observed vertical divergence (~1°), and the counter area. A slightly smaller slit was used in the absolute-intensity measurements to help ensure that all the diffracted intensity was collected in these θ-2θ scans. The relative intensities were then normalized to the absolute-intensity measurements at the two highest temperatures.

It is important to note that in addition to the anharmonic contributions to the (222) reflection, there are weak interactions between neutrons and charged particles in the atom and between the neutron magnetic moments and the electrostatic fields of the atom which can also contribute intensity at the (222). These Foldy[10] and Schwinger[11] corrections are small and have been described in Ref. 3. The neutron data presented here have been corrected for these interactions.

It was expected that the effects of extinction would be small at the (222) owing to the extremely small integrated reflectivities involved (10^{-8} to 10^{-7} rad). At sufficiently small integrated reflectivities, it is well known that the ideally mosaic and perfect-crystal formulations converge to the same solution, resulting in negligible extinction. However, in neutron diffraction, factors of 10^3 in intensity are common between mosaic and perfect crystals. As a result, we decided to investigate possible extinction effects at the weak (222).

We approached extinction in the following manner. Our measurements gave us an experimental number for the integrated reflectivity $R(222) = E\omega/I_0$, where E is the number of neutrons in the peak, ω the angular scan rate, and I_0 the number of neutrons incident per second. We then assumed the crystal was ideally mosaic or perfect and calculated $F(222)$ for each extreme.

The mosaic interpretation was straightforward using the standard kinematic equation

$$R(222) = N^2\lambda^3 F^2(222)[1 - e^{-2\mu t \csc\theta}]/2\mu \sin 2\theta, \quad (1)$$

where N is the number of unit cells per cm^3, t the crystal thickness, and μ the linear absorption coefficient. Our experimentally determined μ was 0.168 cm^{-1} at room temperature and increased approximately 60% over the temperature range.

The perfect formulation was interpreted by numerically integrating the theoretical diffraction curve for a perfect thin crystal with absorption. This was accomplished using the formalism of

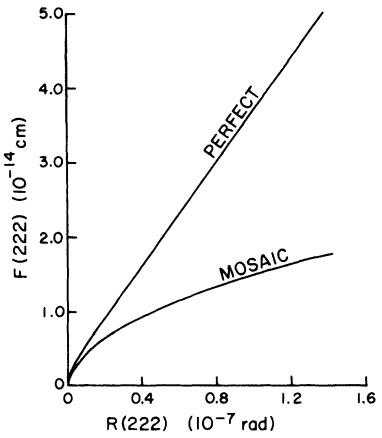

FIG. 3. Theoretical structure factors for ideally perfect and mosaic crystals over our experimental range of absolute integrated intensity. These curves correspond to the germanium neutron case with $\lambda = 2.366$ Å, $t = 1.144$ cm, and $\mu(T)$ as determined experimentally.

James[12] with results similar to those reported by Batterman and Hildebrandt.[13] A computer was used to integrate the equations as a function of $F(222)$ until the appropriate value of $R(222)$ was attained. The results of the calculations (Fig. 3) indicate a substantial difference in F depending on whether the crystal is assumed to be ideally perfect or mosaic at all but the lowest integrated reflectivities observed in these neutron measurements. We present these results to point out that even extremely weak reflections can have important extinction corrections in the neutron case. It should be noted that these considerations were not crucial in the previous silicon (222) neutron measurement,[3] since the precipitation of oxygen in the crystal above 500 °C[14] strained the lattice sufficiently so that the (222) could be interpreted kinematically. However, no such mechanism is characteristic of germanium, and the low-dislocation-crystal results were therefore ambigious.

To check on the presence of extinction, we repeated the measurement of the (222) temperature dependence with a deformed germanium crystal. This sample was originally intended to be a neutron monochromator and had been plastically deformed ~1% at 800 °C. This deformation resulted in a 300-fold increase in the (111) intensity with a mosaic spread of 20′. Accordingly, this crystal was treated as extinction free at the (222). Measurements in transmission with this sample were interpreted using the kinematic Laue equation:

$$R(222) = N^2 e^{-\mu t \sec\theta} \lambda^3 F^2 t/\sin 2\theta \cos\theta . \quad (2)$$

In Fig. 4, we plot the structure factors derived from the reflection measurements of the low-dis-

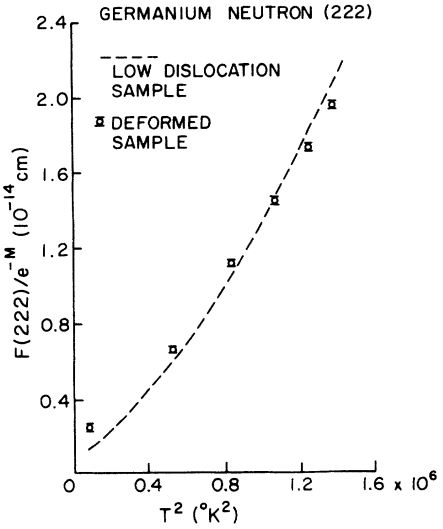

FIG. 4. Germanium neutron structure factor $F(222)/e^{-M}$ vs absolute temperature squared for both a deformed sample (individual data points) and a low-dislocation-density sample (dashed curve). Both sets of structure factors are derived from kinematic diffraction theory and indicate a small departure from a T^2 dependence. The error bars indicate the relative statistical uncertainty in the intensity measurements. Uncertainties in the absolute intensity data are indicated in Table I.

location sample as well as from the transmission measurements from the deformed sample. In each case, the appropriate kinematic equation, (1) or (2) was used. It is apparent that even the low-dislocation sample can be treated kinematically. This is probably due to the fact that extremely high crystal perfection is demanded for a very weak reflection to diffract dynamically. Thermal strains as well as intrinsic defects in the low-dislocation crystal were most likely too large to maintain dynamical conditions.

The higher value of the room-temperature $F(222)$ determined with the deformed sample (as indicated in Fig. 4) may be due to small multiple-diffraction effects resulting from the increased mosaic spread of this crystal. Effects of this magnitude would not contribute significantly at the higher temperatures. However, at room temperature, the lower value of $F(222)$ derived from the low-dislocation sample is probably more accurate. This is a consequence of the negligible mosaic spread in the low-dislocation sample and the insensitivity of the room-temperature structure factor to the perfection of the crystal (see Table I and Fig. 3). At the higher temperatures, where small extinction effects could be present, we take the results from the deformed crystal as the more reliable.

In addition to extinction, another and ultimately more serious experimental problem was discovered while measuring the sample temperature. The same vacuum furnace used in Ref. 3 was used in these germanium measurements. In the course of our investigations on the first germanium crystal, it was noticed that the temperatures at the sample were quite different from those indicated by the controlling thermocouples. The problem was traced to a large thermal drain to the base of the furnace through the control thermocouples. This resulted in indicated temperatures at the control thermocouple being the order of 200 °C too low at a sample temperature of 500 °C, and varying to about 50 °C too low at 1000 °C. For the germanium measurements reported here, the sample temperature was measured with two thermocouples actually embedded in holes in the sample. In the earlier reported silicon measurements,[3] however, the sample was incorrectly assumed to be at the temperature of the control thermocouples. The reported temperature results were therefore in error in the low-temperature regions.

In Fig. 5, we plot the temperature-corrected[15] silicon results together with the earlier results reported in Ref. 3. The low-temperature hump in the $F(222)$ curve as previously reported appears clearly to be an artifact introduced into the data by the errors in temperature measurement. In addition, the over-all shape of the curve is changed and is therefore subject to a slightly different interpretation.

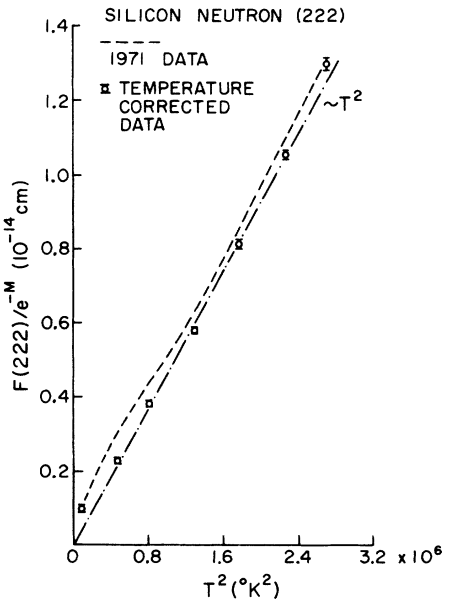

FIG. 5. Temperature-corrected silicon neutron structure factor vs absolute temperature squared. Estimated errors in the relative intensities are shown. The dashed curve represents the incorrect result reported in Ref. 3.

TABLE I. Summary of the germanium and silicon neutron measurements. Values marked with asterisks were determined absolutely and the quoted precision represents absolute statistical errors of one standard deviation. The other values are from normalized relative measurements with relative errors indicated. The germanium results are from the low-dislocation-density sample at room temperature and the deformed sample at higher temperature. All F_{anh} are corrected for Schwinger and Foldy interactions. The β's for silicon differ somewhat from those in Ref. 3 owing to the corrected temperature scale.

Ge(222)			Si(222)		
T (°K)	$F_{anh,\,neut}$ (10^{-14} cm)	β (10^{-12} erg/Å^3)	T (°K)	$F_{anh,\,neut}$ (10^{-14} cm)	β (10^{-12} erg/Å^3)
296	0.124 ± 0.018	2.11 ± 0.33	288	0.070 ± 0.007	5.42 ± 0.54
728	0.585 ± 0.016	1.78 ± 0.05	688	0.185 ± 0.006	2.67 ± 0.08
916	0.966 ± 0.014	1.92 ± 0.04	898	0.316 ± 0.006	2.76 ± 0.06
1032	1.23 ± 0.02	1.97 ± 0.03		*0.311 ± 0.015	*2.71 ± 0.13
1119	1.45 ± 0.02	2.00 ± 0.03	1146	0.477 ± 0.007	2.63 ± 0.04
	*1.44 ± 0.06	*1.99 ± 0.08	1330	0.657 ± 0.014	2.76 ± 0.07
1177	1.63 ± 0.02	2.05 ± 0.03		*0.657 ± 0.007	*2.76 ± 0.04
	*1.64 ± 0.07	*2.06 ± 0.09	1507	0.836 ± 0.010	2.80 ± 0.04
			1649	1.02 ± 0.02	2.91 ± 0.07
				*1.12 ± 0.03	*3.19 ± 0.07

The low-temperature anharmonic $F(222)$ was used to correct silicon x-ray (222) measurements and deduce the temperature dependence of the scattering from the covalent bonds. These results, as reported in Ref. 3, were therefore also affected by the error in temperature measurement. We will postpone further discussion of this until after the results of our current x-ray measurements on germanium and silicon have been presented. The germanium neutron results and the temperature-corrected silicon neutron data are tabulated in Table I.

III. X-RAY EXPERIMENT AND RESULTS

The temperature dependence of the forbidden (222) x-ray reflection in germanium was determined from 23 to 850 °C. The experimental procedure generally followed that of our earlier reported silicon measurement.[5] The measured intensities were put on an absolute scale by measuring the germanium (222) integrated intensity relative to the known silicon (222) reflection. Our previously published silicon measurements[5] were also extended to 800 °C and carefully rechecked over the entire temperature range.

The measurements were carried out on a double-crystal spectrometer of Bond design[16] using Cu $K\alpha$ radiation. We used a germanium monochromating crystal set to diffract from the (220) planes. The diffracted beam from the (222) second crystal was energy analyzed using a solid-state Ge(Li) detector for both the germanium and silicon samples. Contributions from harmonic-wavelength contaminants were found to be small and could easily be excluded by using a scintillation counter with a single channel analyzer set for the $K\alpha$ peak.

Two different low-dislocation-density single crystals of germanium and silicon were used in each of the measurements. The crystals were prepared by orienting and cutting a (111) slice, then grinding the surface on glass to 600-grit SiC, and finally etching the crystals in a solution of 5:3:3 HNO_3, CH_3CO_2H, HF (with a drop of bromine) for several minutes to remove surface damage.

As in the neutron measurements, the crystals were carefully oriented in azimuth to avoid exciting multiple Bragg events. An experimental azimuthal scan at the (222) position for germanium is shown in Fig. 6. This Umweganregung pattern was obtained by positioning the crystal to diffract at the (222) and then rotating the crystal about the normal to the diffracting planes. The Umweganregung-free regions at A and B were used in the germanium measurements. The silicon data were taken in the regions denoted A and B in Ref. 5. The effects of Aufhellung were not observed, although care was taken to avoid Aufhellung positions within these Umweganregung-free regions.

The absolute intensity of the germanium (222) was measured at room temperature relative to the silicon (222). We used our 1970 value of $F(222)$ for silicon (1.46 ± 0.04)[5] which is in excellent agreement with the recent measurements of DeMarco and Weiss (1.44 ± 0.08)[17] and Jennings (1.48 ± 0.03).[18] $F(222)$ for germanium was then calculated using dynamical theory and $\mu_{Si} = 144$ cm^{-1}[18] and $\mu_{Ge} = 352$ cm^{-1}.[19] The dynamical theory was employed since low-dislocation-density samples were used in the measurements. Nevertheless, similar calculations assuming mosaic behavior differ from the dynamic formulation by less than 2%. The difference in sensitivity to perfec-

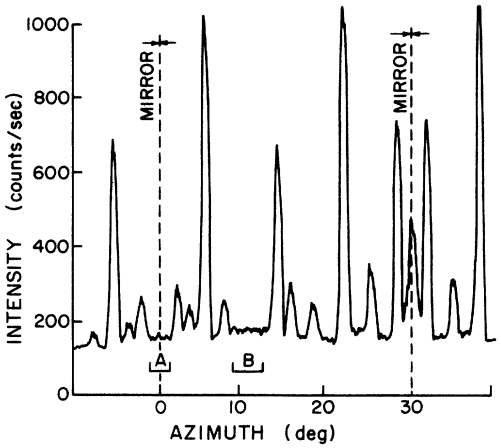

FIG. 6. Variation in x-ray intensity ($\lambda = 1.54$ Å) at the (222) position in germanium as the crystal is rotated in azimuth about the normal to the diffracting planes. "Umweganregung" free regions at A and B were used in the (222) integrated-intensity measurements.

tion between the x-ray and neutron cases is due to the greatly increased absorption for the former.

The actual integrated intensities were measured at A and B azimuths in 180° pairs. The incident intensity was periodically monitored using a polystyrene standard. Approximately ten rocking curves were taken at each azimuth (40 in all) for both the silicon and germanium crystals. These measurements resulted in a room-temperature structure factor $F(222)$ for germanium of 1.06 ± 0.05, with the errors including both statistical deviations and the uncertainty in the silicon $F(222)$. We find that the silicon (222) reflection is a convenient method for determining primary-beam intensity since the intense direct beam is difficult to measure. Furthermore, for our purposes here, the silicon (222) reflection is measured in a geometry closely resembling that used for the germanium (222).

The temperature measurements were carried out in a helium-purged baffle furnace similar to one described previously in the literature.[19] Temperatures were measured with two chromel-alumel thermocouples rigidly mounted to the back of the samples. The intensities returned to their initial room-temperature values after each high-temperature run, indicating negligible surface contamination. In all, approximately 200 000 counts of (222) peak intensity (more in the case of silicon) were taken at each temperature in approximately 30 rocking curves. A typical room-temperature germanium (222) rocking curve is shown in Fig. 7 along with a profile of a similar curve at 787 °C.

The temperature dependence of the x-ray intensities in germanium and silicon (as normalized to the room-temperature intensities) is plotted in Fig. 8. The error bars represent the root-mean-square deviation in the data. It should be noted that the high-temperature data for silicon differs slightly from our 1970 results. The maximum difference is ~4% at 600 °C, or a reduction in F (222) of approximately 2%. We choose to present this more recent data as the more reliable, owing to improved techniques in temperature measurement and an improved experimental configuration which resulted in a greatly increased signal-to-noise ratio and a noticeable improvement in the reproducibility of the silicon (222) measurements. Moreover, the new data cover a wider range in

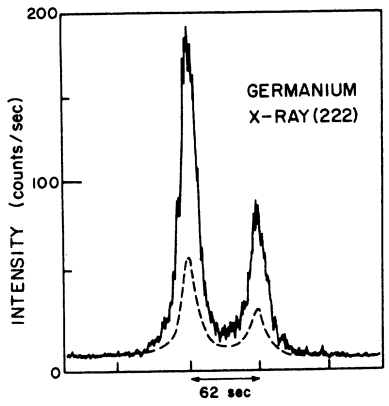

FIG. 7. Typical germanium (222) rocking curves using Cu $K\alpha$ x-rays. The doublet in each peak corresponds to diffraction at the $K\alpha_1$ and $K\alpha_2$ wavelengths. The solid curve represents room temperature data while the dashed curve is for 787 °C.

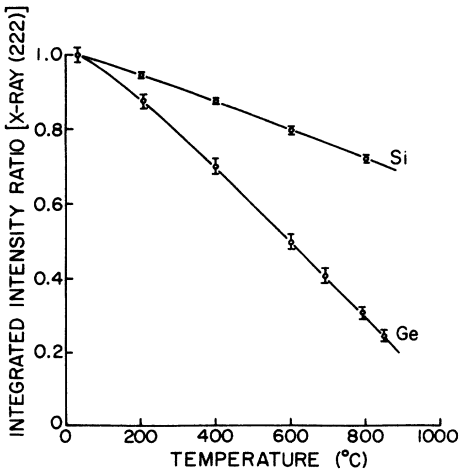

FIG. 8. Observed temperature dependence of the x-ray integrated intensities at the (222) in germanium and silicon as normalized to the room-temperature intensities.

temperature and thus reflects a greater percentage change in measured intensity.

IV. DISCUSSION

Here, as in our earlier publications,[3,5] it is helpful to discuss the effects of anharmonic vibrations in terms of the formalism developed by Dawson and Willis.[2] They consider an Einstein solid in which the individual atoms vibrate in a mean potential of the form

$$V = V_0 + \tfrac{1}{2}\alpha\,(x^2+y^2+z^2) + \beta xyz\,, \tag{3}$$

where α is the harmonic force constant and is related to the Debye–Waller factor and β is the anharmonic force constant. This effective Einstein potential has the required tetrahedral symmetry and represents to lowest order the best approximation to the mean anharmonic potential. A classical ensemble average over this effective potential leads to an expression for the anharmonic structure factor,

$$F(222) = 8ib\,e^{-M}(2\pi/a)^3(\beta/\alpha^3)(hkl)(kT)^2\,, \tag{4}$$

where b is the nuclear scattering length, M the Debye–Waller factor, a the lattice parameter, (hkl) the product of the Miller indices, and kT the product of Boltzmann's constant with the absolute temperature. Assuming that β is a constant, this model predicts a T^2 temperature dependence for $F_{\text{neut}}(222)/e^{-M}$.

We have plotted our experimentally determined $F_{\text{neut}}(222)/e^{-M}$ vs T^2 for germanium and silicon in Fig. 4 and 5. In the case of germanium, the experimental curve departs somewhat from this anticipated T^2 dependence—no straight line drawn through the origin will encompass all the data points. The agreement with the model is better in silicon, although a smaller departure from the T^2 line in the same direction as the germanium departure is apparent.

An indication of the relative importance of anharmonic behavior in silicon and germanium can be obtained by comparing the ratios of the anharmonic to harmonic force constants, β/α, in the two materials. The experimentally determined β's are shown in Table I. These were derived from Eq. (4) using for germanium and silicon, respectively, the lattice parameters[20] $a = 5.658$ and 5.431 Å, the nuclear scattering lengths[21] $b = 0.819\times10^{-12}$ and 0.415×10^{-12} cm, and the harmonic force constants[22] $\alpha = 5.79\times10^{-12}$ and 7.85×10^{-12} erg/Å^2. At the highest temperature, the ratios β/α are 0.35 and 0.37 Å^{-1}, respectively, for germanium and silicon. The relative magnitude of the anharmonic effects is therefore quite comparable in these crystals. Nevertheless, the results suggest a slight difference in the temperature dependence of anharmonicity in silicon and germanium.

The Einstein approach seems quite adequate to describe the essential characteristics of the anharmonic structure factor in both silicon and germanium. The model breaks down, however, when one attempts to explain the anharmonic behavior in detail. One shortcoming is the lack of a first principles method of calculating β. Rough estimates of the magnitude of β can be obtained from thermal expansion,[2,3] but these estimates predict ratios of β/α closer to 0.5 Å^{-1} and are not consistent with the observed temperature dependence. The usefulness of the Dawson and Willis formalism seems to lie in its simplicity. The actual potential involves many-body interactions and is only roughly approximated by Eq. (3).

The anharmonic contributions to the x-ray results are readily deduced by noting that

$$F_{\text{anh, x ray}}(222) = F_{\text{neut}}(222)(f_c/b)\,, \tag{5}$$

where f_c is the x-ray form factor for the core electrons, taken as 8.32 for silicon and 20.9 for germanium.[23] These are the usual free-atom form factors and include dispersion corrections of $+0.2$ and -1.3, respectively.[24] Values of F_{neut} were interpolated at the x-ray temperature points, and then the x-ray structure factors were corrected for the effects of anharmonicity by noting that

$$F_{\text{x ray}}(222) = F_{\text{bond}} - F_{\text{anh}}\,. \tag{6}$$

This resulted in a determination of the temperature dependence of F_{bond}, the structure factor of the valence electrons in silicon and germanium.

In the light of Eqs. (5) and (6), we can now understand the greatly different temperature dependences of the (222) x-ray intensities as shown in Fig. 8. The larger value of f_c in germanium results in a larger F_{anh}, which subtracts an additional temperature-dependent amplitude from the germanium x-ray $F(222)$. It should be pointed out that the determination of $F_{\text{anh, x ray}}$ (and thus F_{bond}) is extremely sensitive to the ratio f_c/b. We used form factors based on free-atom calculations which we expect are quite close to the form factors in the crystal. Nevertheless, at high temperatures in germanium (where F_{anh} is large), the error in F_{bond} due to uncertainties in f_c or b could be significant.

The temperature behavior of F_{bond} in silicon and germanium is shown in Fig. 9 and summarized in Table II. Plotted in the figure are the temperature dependences of the bond structure factors in these crystals as derived from the combined x-ray and neutron measurements. The dashed curves represent the temperature dependence of the core electrons, viz., e^{-M}, the Debye–Waller factor. The simplest conclusion to be drawn from this figure is that for silicon the motions of the bond charge and core electrons are the same up to

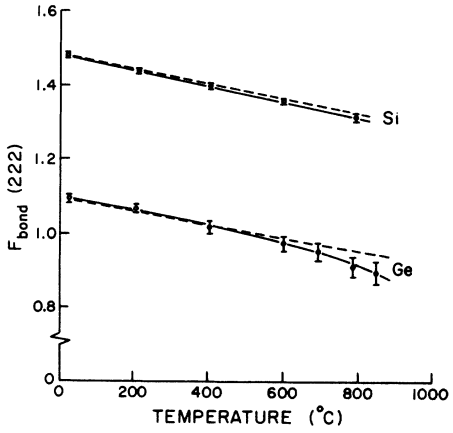

FIG. 9. Observed temperature dependence of F_{bond}, the structure factor for the scattering from the valence electrons, for both Si and Ge.

800 °C while these motions are slightly different for germanium above 700°C. However, the temperature dependence of the bond structure factor can be influenced by not only bond motions, but also by any changes with temperature in the scattering factor for the bonds. We will discuss these two mechanisms in turn.

The effect of atomic vibrations on the intensity of Bragg reflections is well understood,[25] and can be described in terms of the Debye–Waller factor. We can apply the Debye–Waller theory to bond motions by assuming that the covalent bonds can be represented by point charges placed at the midpoint between nearest-neighbor atoms. In this model, then, the motion of the bond can be calculated from the vibrational characteristics of the solid.

If the motions of near neighbors are completely in phase, as would be the case for long-wavelength phonons ($k = 0$), the vibrational amplitude of the bond would be that of the atom. However, as the motion of nearest neighbors becomes more out of phase (as is characteristic of optic modes and short-wavelength acoustic modes), the vibrational amplitude of the bond becomes less than that of the atoms.

An approximate calculation of the bond motion has been carried out by Welch.[26] He considers a Debye model for the separate phonon branches and computes the relative time-dependent positions of near-neighbor atoms. These positions are determined for each phonon and depend solely on the phonon wavelength. The midpoint of these instantaneous positions is considered the vector position of the bond charge. The mean-square amplitude of the bond charge is then calculated by averaging over the three acoustic branches. The optic modes contribute little to the mean-square amplitudes when compared to the acoustic modes even at high temperatures. The preliminary results of model calculations indicate that taking account of the phase difference between near neighbors results in a vibrational amplitude for the bond which is somewhat less than that of the atom.

Although this model suggests a coupled but somewhat reduced vibrational amplitude of the bond with respect to the core, at the present writing the model is not sufficiently refined to draw any detailed conclusions. Therefore, as a basis for comparison with experiment we use the model in which the same Debye–Waller factors are applied to both the bond and core charges. These are based on experimental Debye temperatures of 543 and 290 °K for silicon and germanium, respectively.[27] The temperature dependences predicted from these calculations are indicated with dashed lines in Fig. 9.

Referring to Fig. 9, we see that the experimental silicon F_{bond} agrees very well with this reference e^{-M} dependence over the entire temperature range. This result is in disagreement with the earlier silicon results reported in Ref. 3, where it is suggested that the mean-square amplitude of the bonding electrons is less than that of the core electrons. This suggestion, however, was based in part on silicon x-ray measurements which have since been modified and extended to higher temperatures, as reported in Sec. III. When the present x-ray results are considered in combination with the temperature-corrected neutron measurements (see Sec. II) we are led to a modification of our previous suggestion. If we treat the bond-charge distribution as temperature independent, we conclude that the temperature behavior of the bond in silicon is consistent with a model in which the core and bonding electrons vibrate together with virtually the same amplitude.

The germanium results (Fig. 9) are also in good

TABLE II. Summary of the germanium and silicon x-ray results. The indicated precision in $F_{x\ ray}$ represents the mean-square deviation of the individual relative measurements at each temperature. The absolute errors in the x-ray and neutron measurements were used in scaling the neutron results to the x-ray F_{anh}.

	T (°C)	$F_{x\ ray}$	$F_{anh,\ x\ ray}$	F_{bond}
Ge(222)	23	1.060 ± 0.009	0.032 ± 0.004	1.092 ± 0.010
	208	0.998 ± 0.010	0.069 ± 0.005	1.067 ± 0.011
	401	0.888 ± 0.013	0.128 ± 0.009	1.016 ± 0.016
	600	0.753 ± 0.015	0.221 ± 0.014	0.974 ± 0.021
	693	0.680 ± 0.017	0.273 ± 0.017	0.953 ± 0.024
	787	0.582 ± 0.019	0.329 ± 0.021	0.911 ± 0.028
	850	0.525 ± 0.020	0.373 ± 0.023	0.898 ± 0.030
Si(222)	23	1.460 ± 0.007	0.014 ± 0.002	1.474 ± 0.007
	211	1.414 ± 0.008	0.022 ± 0.002	1.436 ± 0.008
	402	1.355 ± 0.009	0.036 ± 0.002	1.391 ± 0.009
	598	1.297 ± 0.009	0.060 ± 0.002	1.357 ± 0.010
	793	1.229 ± 0.010	0.084 ± 0.003	1.313 ± 0.011

agreement with this e^{-M} dependence up to 700 °C. However, above this temperature, the observed F_{bond} decreases faster than would be expected in the above model, although the difference is not very large. It is important to note that this does not necessarily imply a difference in the behavior of F_{bond} in silicon and germanium. Silicon has a much higher melting point than germanium (1410 vs 937 °C), and based on the ratio of the melting points, such a departure from the e^{-M} reference behavior might not be expected in silicon until well above 800 °C, which is the limit of our experimental x-ray data. Efforts are underway at present to extend the silicon measurements to these higher temperatures.

It is difficult to explain the high-temperature germanium results (Fig. 9) with our model of bond motions. Based on these bond motions alone, the observed high-temperature behavior of F_{bond} in germanium could only be explained if the vibrational amplitude of the bond were greater than that of the core electrons—a rather unphysical situation. This suggests that, at least for germanium, there are contributions to the temperature dependence of the bond structure factor in addition to the effects of bond motions. These additional contributions must be related to changes with temperature in the distribution and/or amount of charge in the bond—i.e., a temperature-dependent scattering factor for the bond.

Ideas along these lines have been proposed by Phillips,[28] who concludes that significant changes in the effective amount of bond charge in silicon should take place in the temperature range investigated.[29] His prediction is that the amount of bond charge will decrease with increasing temperature, effectively reducing the scattering factor for the bond. Such a mechanism could explain the high-temperature germanium results (Fig. 9), and also adds an interesting dimension to the interpretation of the silicon and germanium results in general. It is possible that temperature changes in the bond scattering factors could make significant contributions to the entire observed temperature dependence of F_{bond} in both germanium and silicon. Under these circumstances, the vibrational amplitude of the bond might be considerably less than that of the core electrons, and this is in qualitative agreement with Welch's preliminary calculations.

Without a better theoretical understanding of the nature of the covalent bond in germanium and silicon, it is difficult to discuss the temperature behavior of F_{bond} in more than these general terms. It appears likely that the vibrational amplitude of the bond is somewhat less than that of the core electrons. The influence of temperature changes in the amount or distribution of bond charge seems to be apparent in the high-temperature germanium results and could be present in all the data. As a result, the interpretation of the observed temperature dependence is somewhat ambigious, and definite conclusions concerning the vibrational characteristics of the bonds cannot be drawn at this time.

V. CONCLUSIONS

We have presented the results of a rather extensive study of the temperature dependence of the forbidden (222) reflection in germanium and silicon as measured using both x rays and neutrons. These results have been interpreted in terms of anharmonic atomic motions and the thermal behavior of the covalent bonds in these crystals. Existing theories have accounted for the qualitative aspects of much of the experimental data, but are not adequate to describe our results in detail. We are led to the following conclusions.

(i) The gross features of the observed anharmonic behavior in silicon and germanium are consistent with the single-atom Einstein potential of Dawson.[2] This model, however, fails to account for the detailed temperature dependence of the anharmonic structure factors. The discrepancy between the observed and model-predicted temperature dependence of the anharmonic $F(222)$ is greater in germanium than in silicon, suggesting a slight difference in the anharmonic behavior of these crystals.

(ii) The observed temperature behavior of the scattering from the valence-charge distribution in silicon and germanium is similar to that from the core electrons. This suggests that the vibrational amplitude of the bonds may be comparable to that of the atoms. However, several factors indicate that this may not be the case. Departures from this e^{-M} dependence are experimentally observed in germanium at high temperatures. Furthermore, if the amount of bond charge is decreasing with increasing temperature, as proposed by Phillips, then it follows that the vibrational amplitude of the bond could be less than that of the core electrons which is consistent with Welch's model calculations. The changing of bond charge with temperature could be significant in both the silicon and germanium results, lending considerable range to the interpretation of the temperature dependences in terms of bond motions.

(iii) The over-all qualitative results suggest similarities in silicon and germanium, both in their anharmonic and bonding characteristics. This is consistent with calculations which show that the phonon spectra of these crystals differ essentially by only a scale factor.[30]

Finally, while it is clear that we understand our results in general terms, it is also clear that much of the physics in this study lies in a better inter-

pretation of the quantitative results. This includes both a detailed explanation of the anharmonic behavior and a sorting out of the various contributions to the scattering from the bonds. In particular, the determination of whether the bond-charge motion is the same or different from that of the core electrons will require a better understanding of the temperature dependence of valence-electron wave functions.

ACKNOWLEDGMENTS

The authors wish to express their indebtedness to David Cox of Brookhaven National Laboratory who kindly provided the deformed germanium crystal and to David Welch (also of BNL) for several helpful discussions. We also thank Jerome Hastings of Cornell University who carefully measured the temperature recalibration for the silicon neutron results. In addition, the Cornell authors are appreciative of the hospitality extended to them by Gen Shirane, John Axe, James Hurst, and others associated with the Brookhaven National Laboratory. This work was supported by the U. S. Atomic Energy Commission and the National Science Foundation through the Materials Science Center at Cornell.

---

*Work supported by the U.S. Atomic Energy Commission and the National Science Foundation.

[1]W. H. Bragg, Proc. Phys. Soc. Lond. 33, 304 (1921).
[2]B. Dawson and B. T. M. Willis, Proc. R. Soc. Lond. A 298, 307 (1966).
[3]D. Keating, A. Nunes, B. Batterman, and J. Hastings, Phys. Rev. B 4, 2472 (1971).
[4]J. Roberto, B. Batterman, and D. Keating, Phys. Status Solidi B 59, 59 (1973).
[5]J. B. Roberto and B. W. Batterman, Phys. Rev. B 2, 3220 (1970).
[6]P. Trucano and B. W. Batterman, Phys. Rev. B 6, 3659 (1972).
[7]R. M. Moon and C. G. Shull, Acta Crystallogr. 17, 805 (1964).
[8]H. Cole, F. Chambers, and H. Dunn, Acta Crystallogr. 15, 138 (1962).
[9]G. Shirane and V. J. Minkiewicz, Nucl. Instrum. Methods 79, 109 (1970).
[10]L. L. Foldy, Phys. Rev. 87, 693 (1952).
[11]J. Schwinger, Phys. Rev. 73, 407 (1948).
[12]R. W. James, in *Solid State Physics*, edited by F. Seitz and D. Turnbull (Academic, New York, 1963), Vol. 15, pp. 53–220.
[13]B. W. Batterman and G. Hilderbrandt, Acta Crystallogr. A 24, 150 (1968).
[14]J. R. Patel and B. W. Batterman, J. Appl. Phys. 34, 2716 (1963).
[15]Jerome Hastings kindly performed the actual temperature recalibration.
[16]W. L. Bond, Rev. Sci. Instrum. 39, 1484 (1968).
[17]J. J. DeMarco and R. J. Weiss, Phys. Rev. 137, A 1869 (1965).
[18]L. D. Jennings, J. Appl. Phys. 40, 5038 (1969).
[19]B. W. Batterman, Phys. Rev. 126, 1461 (1962).
[20]D. N. Batchelder and R. O. Simmons, J. Appl. Phys. 36, 2864 (1965).
[21]G. E. Bacon, Acta Crystallogr. A 28, 357 (1972).
[22]Based on the values of θ_M given in Ref. 27.
[23]D. T. Cromer and J. T. Waber, Acta Crystallogr. 18, 104 (1965).
[24]*International Tables for X-Ray Crystallography*, edited by C. MacGillavry, G. Rieck, and K. Lonsdale (Kynoch, Birmingham, 1968), Vol. III, p. 214. It has been brought to the attention of the authors that more recent dispersion corrections are available [D. T. Cromer and D. Liberman, J. Chem. Phys. 53, 1891 (1970)]. If applied to the calculation of $F_{\text{anh, x ray}}$ (Table II), these newer corrections would result in changes in F_{bond} of less than 1% over the entire temperature range in both Ge and Si.
[25]R. W. James, *The Optical Principles of the Diffraction of X-Rays* (Cornell U.P., Ithaca, N.Y., 1965), pp. 193–230.
[26]D. O. Welch (unpublished).
[27]B. W. Batterman and D. R. Chipman, Phys. Rev. 127, 690 (1962).
[28]J. C. Phillips, Phys. Rev. 166, 832 (1968).
[29]J. C. Phillips, Phys. Lett. A 37, 434 (1971).
[30]B. N. Brockhouse, J. Chem. Phys. Solids 8, 400 (1959).